



# Molecular aspects of the activity and inhibition of the FAD-containing monoamine oxidases

Rona Ramsay

Date of deposit	07 05 2019
Document version	Author's accepted manuscript
Access rights	© 2019, Pan Stanford Publishing Ptd Ltd. This work is made available online by kind permission of the publisher. This is the author created, accepted version manuscript following peer review and may differ slightly from the final published version.
Citation for published version	Ramsay, R. (2019). Molecular aspects of the activity and inhibition of the FAD-containing monoamine oxidases. <i>Pharmaceutical Biocatalysis: Fundamentals, Enzyme Inhibitors, and Enzymes in Health and Diseases</i> . vol. 4, Series on Biocatalysis, no. 10, vol. 4, Pan Stanford Publishing Pte. Ltd., Singapore.
Link to published version	<a href="http://www.panstanford.com/books/9789814800617.html#">http://www.panstanford.com/books/9789814800617.html#</a>

Full metadata for this item is available in St Andrews Research Repository at: <https://research-repository.st-andrews.ac.uk/>

St Andrews Research Repository

# **Molecular Aspects of the Activity and Inhibition of the FAD-containing Monoamine Oxidases**

**Rona R. Ramsay**

*University of St Andrews*

*Biomolecular Sciences Building*

*North Haugh, St Andrews KY16 9ST, UK*

[rrr@st-andrews.ac.uk](mailto:rrr@st-andrews.ac.uk)

## **1. Introduction**

### **2. FAD: the catalytic cofactor**

2.1 FAD is covalently attached to MAO

2.3 FAD is modified by irreversible inhibitors

### **3. MAO proteins**

3.1 MAO protein expression and turnover

3.2 MAO A and MAO B structures and active sites

3.3 MAO chemical mechanism

3.4 MAO kinetic mechanism: two-substrate kinetics

### **4. Substrate Specificity of these Promiscuous Enzymes**

4.1 Neurotransmitter metabolism

4.2 Metabolism of biogenic amines

4.3 Products from MAO catalysis

### **5. Inhibition of MAO**

5.1 Reversible inhibitors of MAO

5.2 Examples of tight binding reversible inhibitors of MAO

5.3 Examples of irreversible inhibitors of MAO

### **6. Computational innovation**

6.1 Theoretical elucidation of mechanism

6.2 Data-mining and tools for drug discovery

### **7. Conclusion: the future for MAO inhibition in multi-target drugs**

## 1 Introduction

The flavin-containing monoamine oxidases (MAO, E.C. 1.4.3.4) are redox enzymes found on the mitochondrial outer membrane in every animal cell. Their pharmaceutical importance is due to the fact that MAOs oxidize neurotransmitters such as serotonin and dopamine, changed levels of which are associated with behavioral changes, depression, addiction, aggression and neurodegeneration. High or low MAO activity is associated with pathology. For example, elevated MAO B is observed in neurodegenerative diseases such as Alzheimer's disease. Above average activity of MAO A has been associated with major depression whereas low MAO A is associated with aggression.

MAO inhibitors (MAOI) are widely used as antidepressants, mood stabilizers, and to offset the effects of brain degenerative diseases such as Parkinson's disease. The social and economic impact of neurodegenerative diseases in society remains a good reason for exploring new inhibitors of MAO to elevate remaining neurotransmitters, particularly in multi-target drugs for these complex pathologies. MAO catalysis was first characterized in 1928, but it was the observation of the antidepressant effect of MAOI that triggered the rise of interest in the enzymes in the 1950s (reviewed in (Tipton, 2018)). Figure 1 illustrates the scientific interest in monoamine oxidases expanding during the pharmacological exploration of MAO inhibitors (MAOI) as drugs, mainly used as antidepressants, then beginning to decline in the late 1980s as pharmaceutical interest waned. The publication of the crystal structure of MAO B in 2002 and MAO A in 2005 renewed interest and enabled the modern era of drug design, engaging chemists in particular in discovery of new compounds using computational and high throughput methods (23% of publications from 2005).

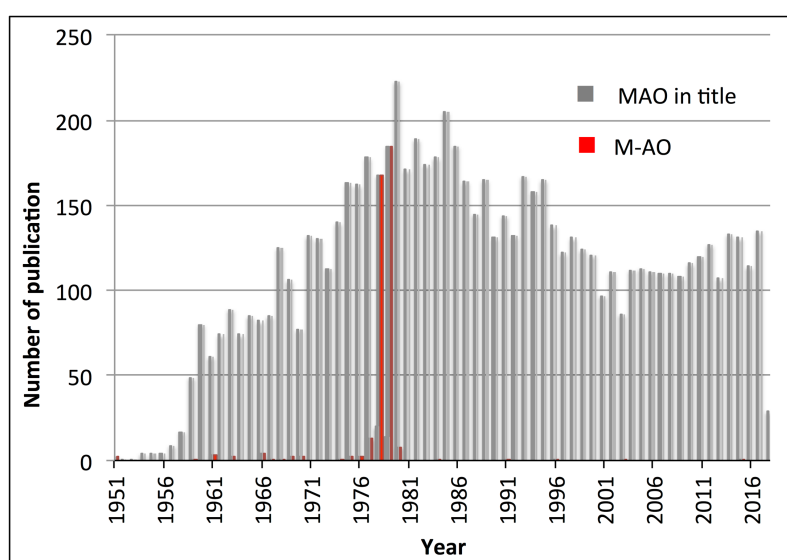


Figure 1. Publications with monoamine oxidase in the title. Note the use of mono-amine oxidase in 1978-79 (compiled from Web of Science, May 2018).

The two monoamine oxidase isoenzymes, MAO A and MAO B, are encoded by genes on the X-chromosome (*MAOA* and *MAOB*) and are expressed in all tissues. In addition to their well-known role in the brain, peripheral MAOs especially in gut (MAO A), liver (both), platelet (MAO B) and placenta (MAO A) play significant roles in protection against biogenic amines and contribute to Phase 1 drug metabolism. In heart, hydrogen peroxide and aldehydes produced by MAO oxidation of amines may contribute to heart failure. These flavoprotein oxidases (E.C. 1.4.3.4) are located on the mitochondrial outer membrane, and therefore metabolise intra-cellular amines. In contrast, the copper-dependent primary amine oxidases (the soluble semicarbazide-sensitive amine oxidase (SSAO) and its membrane form, Vascular Adhesion Protein-1, E.C. 1.4.3.21) act on extra-cellular amines and function in inflammation (Becchi *et al.* , 2017). SSAO, lysyl oxidase (1.4.3.13) and diamine oxidase (E.C. 1.4.3.22 which metabolises histamine) contain 2,4,5-trihydroxyphenylalaninequinone as cofactor ([www.brenda-enzymes.org](http://www.brenda-enzymes.org)). These non-FAD enzymes will not be considered in this article. Other FAD-containing oxidases include the related amino acid oxidases, L-amino acid oxidase (LAAO, E.C. 1.4.3.2) and D-amino acid oxidase (DAAO, E.C. 1.4.3.3), and spermine metabolising enzyme, polyamine oxidase (E.C. 1.5.3.13), all of which have covalently bound FAD. A possible evolutionary precursor of MAO is found in the peroxisomes of *Aspergillus niger* and has a non-covalently bound FAD co-factor (Sablin *et al.* , 1998) making it interesting for chemical applications (Bailey *et al.* , 2007).

The reaction catalysed by MAO moves two hydrogen atoms to the FAD from the amine forming an imine. The reduced FAD is then reoxidized by oxygen to form hydrogen peroxide. The imine product is then hydrolysed by water giving the corresponding aldehyde and ammonia (Fig. 2). This chapter will consider the structure of the enzyme and the redox reaction with the cofactor and before turning to the substrate specificity, kinetics and mechanism that are important for drug design. MAO A and MAO B show broad specificity for both substrates and inhibitors, yet can display exquisite selectivity as will be discussed in the last section on inhibitors.

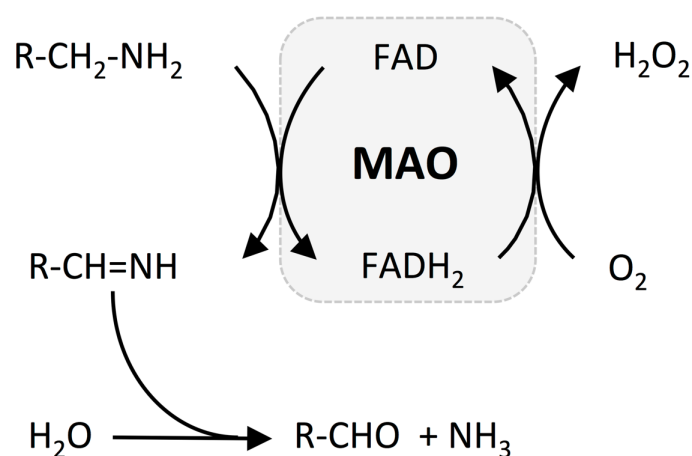


Figure 2 The redox reaction catalysed by MAO is followed by spontaneous hydrolysis of the imine product to give the aldehyde and ammonia. The FADH<sub>2</sub> is reoxidized by oxygen to give the second product, hydrogen peroxide.

## 2 FAD: the catalytic cofactor

### 2.1 FAD is covalently attached to MAO

FAD, a redox cofactor important for catalysis in many enzymes, is derived from the vitamin riboflavin. As in most many FAD-containing enzymes, the adenine part of the molecule binds to a Rossmann fold in the protein. The isoalloxazine ring part of FAD is held in position by a covalently bond to a cysteine residue in MAO (Fig. 3). In all crystal structures of MAO B, the isoalloxazine ring is bent by about 30° (Binda *et al.*, 2003) with about 0.3° difference between the oxidized and reduced forms. However, molecular dynamics has now enabled a more realistic picture of the shape of the flavin in the flexible protein active site. Two different studies have shown that it is almost planar in the oxidised form (FAD) (Vianello *et al.*, 2012, Zapata-Torres *et al.*, 2015), but when it is reduced either by a hydride ion from the substrate transferred to N5 in the first step of the catalytic mechanism or after the propargylamine adduct has formed at N5, the FADH<sub>2</sub> is bent by almost 30 degrees (Borstnar *et al.*, 2011) in agreement with the crystal structure.

Covalent attachment (at the C8 position of FAD in MAO), bending, and the surrounding protein groups alter the redox potential in flavoproteins. The two-electron redox potential for FAD in solution is -0.23 V and is the similar for the cysteinyl-FAD in MAO (about -0.2 V). The redox potential for amine oxidation is greater than +1 V, so for amine to reduce MAO requires a large adjustment from binding to the protein. FADH<sub>2</sub> readily reacts with oxygen producing hydrogen peroxide (H<sub>2</sub>O<sub>2</sub>) (+0.3 V). In amine oxidases, the reoxidation is thought to proceed via a C4a hydroperoxy intermediate (Mattevi, 2006). Although the catalytic reaction is a two-electron reduction, with hydride transfer the most likely mechanism, FAD is a versatile one or two electron acceptor. When MAO is reduced by dithionite in the presence of mediator dyes, inhibitors stabilize the anionic semiquinone form (Hynson *et al.*, 2004).

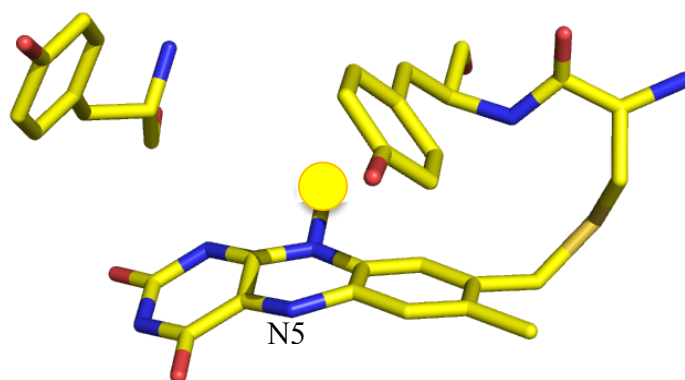


Figure 3 The 8- $\alpha$ -S-cysteinyl-isoalloxazine ring of FAD in the active site of MAO. The yellow circle at N10 indicates the rest of the FAD molecule. In MAO B (pdb: 1GOS), the flavin is bonded to Cys397 and the two

tyrosines that are key to the aromatic cage for the substrate are Tyr398 and Tyr 435. The N5 (labelled) is involved in catalysis of the redox reaction.

## 2.2 FAD is modified by irreversible inhibitors

The major pharmaceutical drugs used to inhibit MAO modify the FAD irreversibly. Phenelzine (Nardil), tranylcypromine, and deprenyl (Selegiline) represent three classes of MAO inactivators, all of which form a covalent bond to the N5 of FAD as shown in Fig 4. Phenelzine and tranylcypromine are successful antidepressants achieving about 50% response rates, slightly better than the tricyclic antidepressants (Nutt, 2006). Deprenyl is now used in both oral and patch formulations both to delay the need for L-DOPA and as adjunct therapy in Parkinson's disease. Although the structures of these MAO-inhibitor adducts were characterized chemically and by the crystal structures, the mechanisms of adduct formation remain incompletely understood. Inhibition of MAO will be discussed in more detail below.

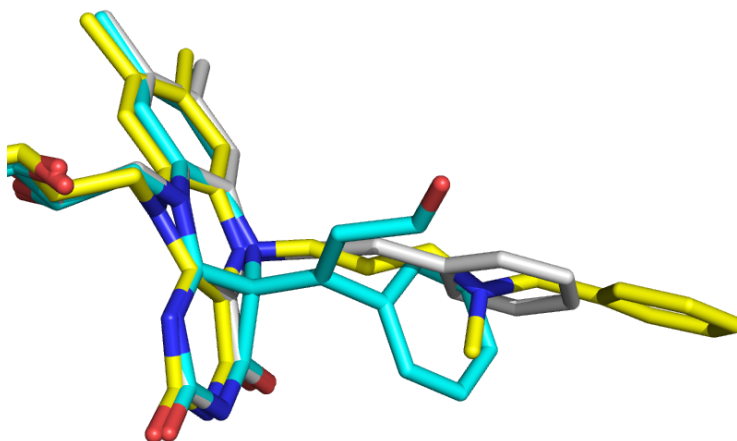


Figure 4 Irreversible MAO inhibitor drugs all form the N5 adduct with the flavin. The figure was prepared in MACPyMol with the protein main chains aligned. The adducts shown are MAO B with phenelzine (grey, 2VRM), and deprenyl (1GOS) bonded to N5, and tranylcypromine (cyan, 2XFU) bonded at C4a of the FAD.

## 3. MAO proteins

### 3.1 MAO protein expression and activity

Abnormal MAO activity has long been associated with neuropathology and behavioural changes (Finberg and Rabey, 2016). Humans with low MAO A activity and MAO A knockout mice display aggression (Bortolato and Shih, 2011). Low platelet MAO B is associated with alcoholism and behavioural disinhibition (van Amsterdam *et al.*, 2006, Bortolato and Shih, 2011). Expression of MAO A and B differs by cell type and they are regulated differently. The upstream 30 base pair

VTNR polymorphism in the MAO A promoter with 3 or 5 repeats results in as much as a 10-fold lower expression compared to the normal 4 repeats (Sabol *et al.* , 1998), and a downstream VTNR has been reported to decrease expression of a novel isoform (Manca *et al.* , 2018). Both MAO A and B have similar GC-rich promoter regions activated via Sp1 sites. Both promoters are down-regulated by the transcription factor R1 but MAO A expression is increased via the Glucagon Receptor Element and MAO B expression is increased by retinoic acid (Shih *et al.* , 2011).

Epigenetic regulation also plays a role and may provide the link with environmental influence on behaviour. One study demonstrated that MAOA promoter hypermethylation was associated with antisocial personality disorder and with high serotonin levels via down-regulation of MAO A gene expression (Checknita *et al.* , 2015). Epigenetic influence was explored using allelic expression imbalance (AEI) of two single nucleotide polymorphisms in female human brain tissue. AEI ratios varied from 0.3 to 4 in prefrontal cortex samples indicating transcription-level regulation of mRNA production. CpG methylation in the MAOA promoter region was high in females and the extent of allelic MAOA methylation correlated with AEI ratio, showing that CpG methylation regulates gene expression (Pinsonneault *et al.* , 2006). Using molecular biology combined with Positron Emission Tomography (PET) to measure regional MAO activity, a robust association of CpG site-specific methylation of the MAOA promoter with regional brain MAO A levels was demonstrated, strongly supporting the notion that epigenetic status (which can be influenced by environment, such as smoking) contributes to inter-individual differences in behaviour (Shumay *et al.* , 2012).

The activity of MAO in human brain studied by PET has confirmed earlier studies that recovery of MAO activity after inhibition by irreversible inhibitors such as deprenyl is slow, with a half-life of 40 days in the human brain, because it depends on the replacement of the inactive adduct enzyme with newly synthesized protein. PET has also proved useful for dosing studies, indicating that more than 75% occupancy of MAO active sites is required for clinical efficacy (reviewed in (Fowler *et al.* , 2005)).

### **3.2 Structures and Active Sites**

The first purified MAO B was extracted from beef liver (Salach, 1979) and MAO A from human placenta. The first large scale heterologous expression of MAO A in *S. cerevisiae* provided pure enzyme for kinetic studies (Weyler *et al.* , 1990), but it was high-level expression in *Pichia pastoris* (Newton-Vinson *et al.* , 2000, Li *et al.* , 2002) that enabled crystallization first of human MAO B protein, and then of rat and human MAO A (Binda *et al.* , 2002, Ma *et al.* , 2004, De Colibus *et al.* , 2005, Son *et al.* , 2008). The terminal hydrophobic helix of each of the two subunits of MAO is monotonically inserted in the mitochondrial outer membrane and further residues associate with the surface of the membrane, so that high amounts of detergent are required to solubilize the protein. The active site details from the crystal structures opened the way for structure-based drug design.

Comparison of the rat and human MAO structures revealed minor differences reflecting the reported species differences in substrate and inhibitor specificity (Krueger *et al.*, 1995, Hubalek *et al.*, 2005, Ramadan *et al.*, 2007). In all structures, the catalytic FAD is at the end of a tunnel leading from the surface of the protein. The tunnel is generally hydrophobic, ending in an aromatic cage near the flavin where tyrosines (Tyr398 and Tyr435 in MAO B) align the neutral amine substrate towards the C4-N5 region of the flavin. The flavin is bent at about 30° along the N5-N10 axis favoring reduction as shown in Fig. 3, and there is a lysine-water-flavin(N5) motif important for the redox reactions of the flavin (Binda *et al.*, 2002).

The two MAOs share 70% sequence identity but the active sites have subtle differences. In particular, MAO B has a constriction in the middle of the cavity due to residues isoleucine 199 and tyrosine 326 and MAO B has one cysteine (Cys172) not present in the MAO A active site (Edmondson *et al.*, 2007, Milczek *et al.*, 2011, Orru *et al.*, 2013). The differences allow discovery or design of compounds for selective inhibition, as will be discussed in the inhibition section.

### 3.3 MAO chemical mechanism

Supported by extensive molecular model chemistry and recent thermodynamic calculations, three mechanisms have been considered for MAO catalysis: the polar nucleophilic mechanism (Orru *et al.*, 2013), the radical (Silverman, 1995), and the hydride transfer mechanism (Kay *et al.*, 2007). The hydride transfer mechanism (Fig. 5) is found in other oxidases and is supported by theoretical studies based on transition state theory (Vianello *et al.*, 2016). However, the versatility of flavin catalysis could allow alternative mechanisms with specific chemicals, for example with the cyclopropylamines.

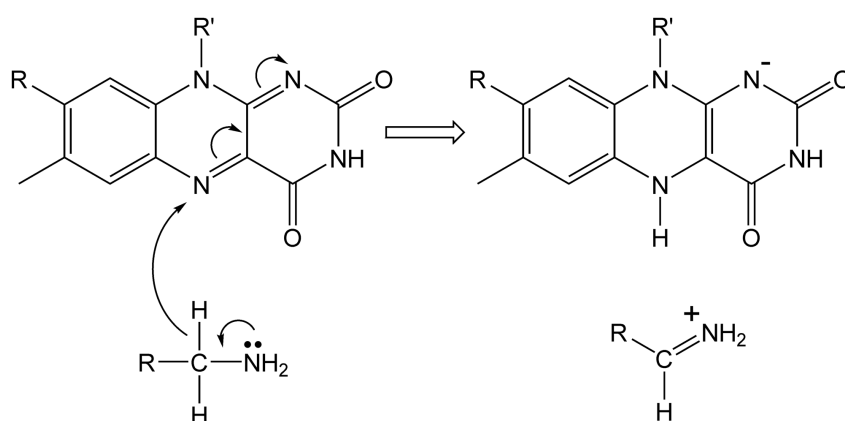
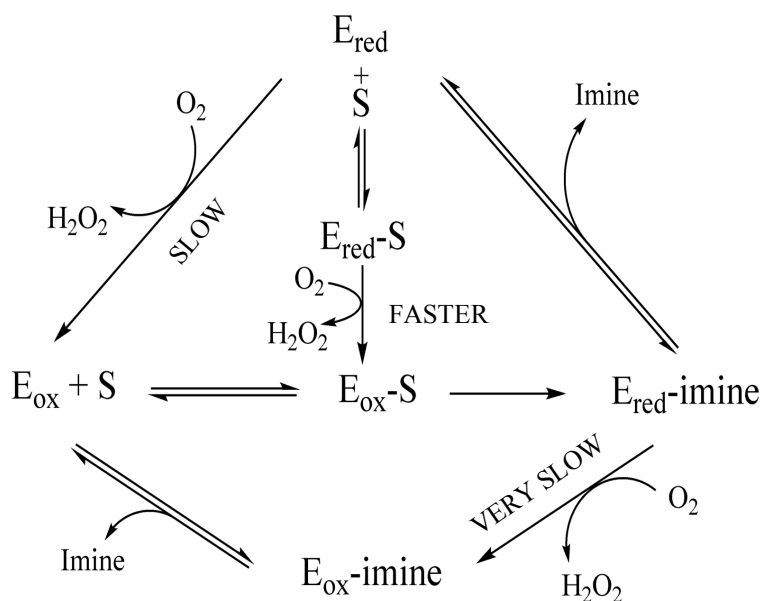


Figure 5 Hydride transfer is a probable mechanism for amine oxidation by MAO

### 3.4 Two Substrate Kinetics and Consequences for Amine Turnover

MAO catalyzes the oxidation of amines by molecular oxygen. Depending on the conditions used, this two-substrate enzyme can reveal either ping-pong kinetics or a ternary complex kinetic mechanism in which a new amine substrate molecule binds to the reduced MAO before reaction with

oxygen (Tan and Ramsay, 1993). **Fig. 6** illustrates the three possible re-oxidation pathways.



**Figure 6** The catalytic cycle in MAO showing the alternative pathways for re-oxidation of FAD.

Both steady-state and stopped flow kinetics have been used to establish that ligands (substrate or inhibitor) can bind to either the oxidized or reduced forms of the enzyme, albeit with very different affinities (Tan and Ramsay, 1993, Ramsay *et al.*, 2011). The proportion of MAO in the reduced state will vary depending on the amine concentration, the rates of reduction and oxidation of the flavin, and on the oxygen levels. Thus, the turnover of amines *in vivo* will be influenced by the local concentration of oxygen and by the redox state of the enzyme in the presence of the predominant substrate (Ramsay, 1998, Sablin and Ramsay, 2001). For MAO A, the rates of the reductive half reaction ( $k_{red}$ ) are all similar to the steady-state rate ( $k_{cat}$ ), and the oxidative half reaction in the presence of amine is faster ( $k_{ox}$ ). For MAO B, the rate of amine oxidation can be faster than  $k_{cat}$ . For some substrates, notably phenylethylamine, the oxidative half-reaction determines the rate of turnover (**Table 1**). These rates mean that MAO A oxidizing PEA will be predominantly oxidized but MAO B will be fully reduced in the steady state. Another important difference between MAO A and B is the  $K_M$  for oxygen. MAO A continues working at low oxygen concentration ( $K_M = 0.06$  mM) whereas MAO B has a  $K_M$  close the concentration of dissolve oxygen (0.28 mM), so that the rate of MAO B catalysis will decrease with the oxygen concentration in the cell.

**Table 1** Rates for turnover ( $k_{cat}$ ), reductive half-reaction ( $k_{red}$ ), and the oxidative half reaction in the presence of amine ( $k_{ox}$ ) in purified MAO A and MAO B. The data are taken from (Tan and Ramsay, 1993).

Amine	MAO A rates (min <sup>-1</sup> )			MAO B rates (min <sup>-1</sup> )		
	k <sub>cat</sub>	k <sub>red</sub>	k <sub>ox</sub>	k <sub>cat</sub>	k <sub>red</sub>	k <sub>ox</sub>
5HT	2.8	2.1	6	0.08	0.1	2
PEA	0.75	1.10	12	3.6	572	2
MPTP	0.20	0.20	40	0.16	0.12	6
No amine			1			1

## 4. Substrate Specificity of these Promiscuous Enzymes

### 4.1 Neurotransmitter metabolism

Substrate specificity depends not only on the  $k_{cat}$  discussed above but also on the recognition of the substrate by the enzyme, measured in kinetic terms by  $K_M$ . For example, the  $K_M$  for serotonin in rat brain homogenates is 0.18 mM with MAO A but is 1.2 mM with MAO B so clearly serotonin concentrations would have to be very high before MAO B contributed much to its metabolism. Comparison of specificity is best informed by  $k_{cat}/K_M$  alongside the expected or measured concentrations in the cell. Some values for  $k_{cat}/K_M$  in rat brain are given in [Table 2](#). Note that the location of MAO on the mitochondrial surface means that it is the intracellular concentration of amine that is important rather than the synaptic concentration. Reuptake systems bring the extracellular amine into the presynaptic nerve terminal where mitochondria are clustered and the storage vesicles are also located. The vesicular reuptake system (VMAT2) with affinity for the monoamine neurotransmitters of 1.4  $\mu$ M for dopamine and 0.9  $\mu$ M for serotonin (Erickson *et al.*, 1996) efficiently clears dopamine to leave cytosolic levels below 50 nM (Mosharov *et al.*, 2006, Mosharov *et al.*, 2009). The MAO that predominates in dopaminergic neurons is MAO A with a  $K_M$  for dopamine of 212  $\mu$ M. In serotonergic cells, MAO B predominates with a  $K_M$  for serotonin of 1 mM (Youdim *et al.*, 2006). Thus most of the neurotransmitters will be returned to storage vesicles and only a very little metabolized. However, inhibition of MAO B in particular raises the overall content of amines in the brain. MAO B is the major form in all the non-neuronal cells and has been reported to increase with aging and in Alzheimer's disease, making it an attractive pharmaceutical target to help maintain global levels of amines outside the synapses in deteriorating brain. The importance of MAO for metabolism of neurotransmitter is apparent in serotonin toxicity where excessive levels of extracellular serotonin accumulate. It occurs only when a serotonin reuptake inhibitor is co-administered with a non-selective irreversible MAOI (Gillman, 2011).

**Table 2 Relative rates of amine oxidation by rat MAO A and MAO B**

Calculated from (Fowler and Tipton, 1984).

Substrate	Catalytic constant ( $V/K_M$ ) $\mu\text{mol. min}^{-1}.\text{mg}^{-1}.\text{mM}^{-1}$	
	MAO A	MAO B
Serotonin	540	7
Tyramine	309	113
Phenylethylamine	46	4350
Dopamine	231	232
Noradrenaline	232	143

## 4.2 Metabolism of biogenic amines

MAO enzymes in the periphery are important for metabolism of exogenous amine compounds. Ingested amines have variable proportions present as the neutral compound that can diffuse cross membranes. Where there is a pH difference, such as between cytosol and the mitochondrial matrix, reprotonation results in accumulation of the charged species in the new compartment. The mitochondrial transmembrane potential also favors retention of positively charged amines. Biogenic amines from the diet, principally tyramine, are extensively metabolized in the intestinal wall by MAO A (Anderson *et al.*, 1993). If tyramine increases in the circulation, complex sympathetic nervous system perturbations ensue, with consequent vasoconstriction and bradycardia (reviewed in (Finberg and Gillman, 2011)). Tyramine accumulation results in this “cheese effect” when MAO A in the gut and MAO A and MAO B in the liver are inhibited by non-selective drugs such as tranylcypromine or phenelzine. The tyramine-induced cheese effect is avoided by using selective MAO B inhibitors such as selegiline in adjunct therapy of Parkinson’s disease or reversible inhibitors of MAO A in depression (Lum and Stahl, 2012).

A wide variety of amine-containing drugs are also metabolized by MAO, contributing 1% of the enzymatic metabolism of marketed drugs (compared to 95% by the P450 family) (Rendic and Guengerich, 2015). The biotransformation of drugs and other xenobiotics by the amine oxidases in contrast to the P450 family has been reviewed (Benedetti *et al.*, 2001). Metabolism by MAO can also transform a compound into a toxic product. A well-known example is the four electron oxidation of 1-methyl-4-phenyl-1,2,3,6-tetrahydropyridine (MPTP) by MAO to 1-methyl-4-phenylpyridinium (MPP<sup>+</sup>). The toxic MPP<sup>+</sup> is taken up into dopaminergic cells in the substantia nigra and is accumulated into mitochondria where it inhibits NADH oxidation by the respiratory chain, hence preventing ATP production and consequent dopaminergic cell death leading to Parkinson’s disease (Singer and Ramsay, 1990). To avoid such adverse side effects in development of new compounds, computational methods for the prediction of probable metabolic products has been developed based on databases of approved drugs with well-characterized metabolic profiles (Kar and Leszczynski, 2017).

### 4.3 Products from MAO catalysis

All amine substrates are oxidized by MAO to the imine which is hydrolysed non-enzymically to the corresponding aldehyde (Fig. 1). Aldehydes are somewhat reactive molecules that can damage biological molecules by nucleophilic addition. In the cell, aldehyde dehydrogenase metabolizes the aldehyde to the carboxylic acid. The second product of MAO catalysis is hydrogen peroxide (H<sub>2</sub>O<sub>2</sub>). The toxic effect of MAO-generated H<sub>2</sub>O<sub>2</sub> was clearly demonstrate for serotonin metabolism in heart (Pena-Silva *et al.* , 2009). Decreased generation of H<sub>2</sub>O<sub>2</sub> in the brain may contribute to the beneficial effects of selegiline.

## 5. Inhibition of MAO

The pharmacological exploitation of MAO inhibitors as drugs began with the serendipitous discovery that the tubercular drug iproniazid had antidepressant effects (reviewed in (Tipton, 2018)). Despite the cheese effect of the non-selective irreversible inhibitors, the most effect MAO inhibition is still achieved by irreversible inhibition. Drugs such as pargyline and tranylcypromine are underused in psychiatry, yet the reversible MAO A-selective antidepressant drug, moclobemide, works only in some cases of depression. MAO B-selective reversible inhibitors have been slow to appear but safinamide (K<sub>i</sub> for MAO B 450 nM) has now been approved by the FDA for use as adjunct therapy in Parkinson's disease. The therapeutic potential of MAOI is clearly recognized (Youdim *et al.*, 2006), with more recent efforts yielding patents for new reversible inhibitors or for inhibitors that also target other features of degenerative disease (multi-target compounds) as will be discussed below.

**Table 3. Reversible and irreversible inhibition of MAO**

Type	Reaction	Measure	Comment
Reversible	$E + I \xrightleftharpoons[k_{-1}]{k_{+1}} E \cdot I$	$K_i = k_{-1}/k_{+1}$	Reversible binding can be at equilibrium, or slow, or tight, depending on rates
Irreversible (mechanism-based)	$E + I \xrightleftharpoons[k_{-1}]{k_{+1}} E \cdot I \xrightarrow{k_{+3}} E-I$	$K_i$ and $k_{inact}$	Depends on binding, catalytic conversion of I, and then chemical reaction

The definitions used for assessment of reversible and irreversible inhibitors discussed here are given in [Table 3](#). The best pharmacological approach for MAO inhibition is not clear. Proven history of over 50 years has established the effectiveness of irreversible drugs such as selegiline. Extensive

human studies *in vivo* over the last 20 years using PET have established that 75-80% inhibition of MAO is required before beneficial effects are seen, emphasizing the spare capacity in this enzyme (Fowler *et al.* , 2015a). With irreversible inhibition the effective inhibition is long lasting, with slow resynthesis of MAO to replace the inactivated enzyme. Selective irreversible inhibitors of MAO B (for example, selegiline) now have a proven safety record, improved by delivery in transdermal patches to avoid major inhibition of MAO B in the liver. Reversible inhibitors require constant dosing, and even they are not completely free of the cheese effect (Lum and Stahl, 2012). The inhibition of MAO increases brain neuroamines, but the subsequent downstream changes in receptors and heterologous effects on other neurotransmitter systems are slow. Thus, the prolonged effect of irreversible inhibition may be more suited to this set of events. The sections below consider key reversible inhibitors, effective tight-binding inhibitors and irreversible inhibitors in turn before looking briefly at new computational approaches to drug discovery.

### 5.1 Reversible inhibitors of MAO

The reluctance to prescribe irreversible inhibitors for neuropathology because of the cheese effect has supported extensive exploration of new scaffolds by medicinal chemists. Aspects of the reversible inhibition from structure-activity studies were reviewed before the publication of the crystal structure of the enzymes (Wouters, 1998). More recently, many compounds, mostly with common features of at least one aromatic ring and a nitrogen atom, and having a relatively linear structure, have been discovered through data mining or by structure-based design. A recent review pulls together the many chemical entities that can inhibit reversibly and selectively MAO A or MAO B (Tripathi *et al.* , 2018). Of particular interest are the various derivatives based on the coumarin scaffold, for use as multi-target compounds against neurodegeneration (reviewed in (Stefanachi *et al.* , 2018)). Many medicinal chemistry groups are aiming to develop other MAO-A and MAO-B reversible inhibitors, only some of which reach the stage of pharmacology (Finberg and Rabey, 2016). In light of the growing scale of neurodegenerative disease, promising compounds are promptly patented, and patent updates appear regularly, such as one surveying patents of clinical interest filed in 2015-2017 (Carradori *et al.* , 2018). These patents include 108 compounds, both synthetic and from natural sources, including coumarins, pyrazoles, and arylamides.

The initial experimental assessment of novel reversible inhibitors is usually done by determining the  $IC_{50}$  values of a series of chemicals. The two-substrate, alternative pathway kinetics described above means that great care is required to set conditions that allow measurement of competition with the amine substrate: ie, that the amine substrate is rate limiting. For comparison of inhibition of MAO A and MAO B, the fractional saturation with amine substrate should be the same (usually 2 or 3 times  $K_M$ ). Further details can be found elsewhere (Ramsay *et al.*, 2011, Ramsay and Tipton, 2017). Compounds of interest are then characterized to confirm reversibility and identify mode of inhibition.

Most inhibitors are competitive with the amine substrate, as can be understood by inspection of the active site: both substrate and inhibitor bind in the same place. However, apparent deviation from competitive inhibition is sometimes found for MAO B. The MAO B  $K_M$  for oxygen of 0.23 mM is close to the concentration of oxygen in air-saturated buffer at 37°C. The deviations can arise when the conditions chosen result in both oxidized and reduced MAO B being present in the steady state, so that the affinity of the compound for both forms influences the shape and concentration-dependence of the dose-response curve (Ramsay *et al.*, 2011).

The one clear example of mixed inhibition that has been fully established is for the imidazoline compound 2-(2-benzofuranyl)-2-imidazoline (2-BFI). The 2-BFI binds in the entrance cavity of MAO B when the cavity is in a particular conformation that can be stabilized by tranlylcypromine bound in the catalytic site (Bonivento *et al.* , 2010, McDonald *et al.* , 2010). The I<sub>2</sub>-type imidazoline compounds bind to a subset of MAO molecules with nanmolar affinity but inhibition of the bulk population of MAO requires micromolar concentrations (Jones *et al.* , 2007, McDonald *et al.*, 2010). The significance of imidazoline binding to MAO in the cell is not clear.

## 5.2 Examples of tight binding reversible inhibitors of MAO

The rate of binding of harmine to MAO measured by rapid scan stopped-flow spectrometry was  $2 \times 10^8 \text{ M}^{-1} \text{ s}^{-1}$ , close to diffusion-limited rate. Yet the onset of inhibition in a steady-state assay required almost 2 minutes. Many inhibition studies preincubate the ligand and enzyme for 5 -30 min before adding substrate to start the reaction. This allows equilibrium of the inhibitor in the absence of substrate (binding affinity) but if the off-rate is slow, curvature of the time course in the presence of substrate will be observed. Thus, continuous assays with or without preincubation can give additional information. The harmine on-rate is fast, so its off-rate must be slower giving the tight-binding  $K_i$  of 5 nM (Kim *et al.* , 1997).

The thionine dye, Methylene Blue also binds tightly to MAO A. Clinical uses (surgical, antimalarial) and preclinical information on the dye, methylene Blue (MB) have recently been reviewed (Delpont *et al.* , 2017). MB inhibits nitric oxide synthase, guanyl cyclase and MAO A, the latter with a  $K_i$  of 28 nM (Table 4). Its potency as an MAO inhibitor *in vivo* became evident as a result of serotonin syndrome, sometime fatal when it was administered during surgery to patients taking serotonin reuptake inhibitor antidepressants (Gillman, 2006). MB also acted as an electron donor and acceptor with MAO A (Ramsay *et al.* , 2007) as it does in mitochondria (Delpont *et al.*, 2017).

Safinamide binds tightly to MAO B but also blocks voltage-gated sodium and calcium channels, and inhibits glutamate release in rat hippocampal synaptosomes (Caccia *et al.* , 2006, Stocchi *et al.* , 2006). Safinamide, a selective reversible inhibitor of MAO B (Table 4, (Binda *et al.*, 2007), was used to explore the structural effect of the two residues specific to the active site of MAO B. Isoleucine 119

and tyrosine 326 constrict the cavity of MAO B into entrance and catalytic parts whereas MAO A does not have this “gate”. Long ligands such as safinamide span this gate, pushing it “open” and flexing around the constriction. MAO A has a wider active site without this constriction so that safinamide binds poorly ( $K_i = 365 \mu\text{M}$ , Table 4). The strong inhibition of MAO B by safinamide was increased from 450 nM to 21 nM after the mutation to alanine of Ile199, one of the gating residues between the entrance and catalytic cavities of MAO B. However, in the double mutant, Ile199Ala-Tyr326Ala, affinity was much less ( $K_i = 4 \mu\text{M}$  (Milczek *et al.*, 2011)).

**Table 4** Examples of drugs that inhibit human MAO A and MAO B

Drug	Indication	MAO A $K_i$ ( $\mu\text{M}$ )	MAO B $K_i$ ( $\mu\text{M}$ )	Reference
<b>Reversible</b>				
D-Amphetamine	Controlled	18	250	(Ramsay and Hunter, 2002)
Harmine	Endogenous	0.005	121 <sup>a</sup>	(Kim <i>et al.</i> , 1997, Reniers <i>et al.</i> , 2011)
Methylene Blue	Trial AD	0.028	5.5	(Ramsay <i>et al.</i> , 2007)
Moclobemide	Depression	11.5	>100	(Da Prada <i>et al.</i> , 1989, Curet <i>et al.</i> , 1996)
Pirlindole	Depression	0.045	>100	(Medvedev <i>et al.</i> , 1999)
Safinamide	PD adjunct	365	0.45	(Binda <i>et al.</i> , 2007)
<b>Irreversible</b>		<b>IC<sub>50</sub><sup>b</sup> (<math>\mu\text{M}</math>)</b>	<b>IC<sub>50</sub><sup>b</sup> (<math>\mu\text{M}</math>)</b>	
Clorgyline	Imaging	0.0004	3.57	(Malcomson <i>et al.</i> , 2015)
Deprenyl (Selegiline)	PD adjunct	16.9	0.004	Unpublished <sup>c</sup>
Pargyline	Depression	2.47	0.0077	Unpublished <sup>c</sup>
Tranlycypromine	Depression	0.237	0.074	(Malcomson <i>et al.</i> , 2015)
Phenelzine	Depression	4.50	9	(Binda <i>et al.</i> , 2008)
Isocarboxid <sup>d</sup>	Depression	0.3	0.18	(Da Prada <i>et al.</i> , 1989)

<sup>a</sup> Estimate from invalid use of Cheng-Prusoff equation. <sup>b</sup>IC<sub>50</sub> values from different labs show considerable variation. <sup>c</sup>In the unpublished data, activity was measured, using 1 mM tyramine as substrate, after 30 minutes pre-incubation of MAO with the inhibitor. (P.L. Joffrin (2016) Honours Thesis, University of St Andrews). <sup>d</sup>Rat brain – the reference also includes values for some of the other irreversible inhibitors in rat brain homogenates.

### 5.3 Examples of irreversible inhibitors of MAO

Table 4 lists the irreversible inhibitors of MAO in clinical use. The three major classes of drugs that form covalent adducts with MAO are the older hydrazines (phenelzine, isocarboxazid), a cyclopropylamine (tranylcypromine), and the propargylamines (pargyline, clorgyline, deprenyl). The general scheme in Fig. 7 shows initial enzyme-catalyzed oxidation of the inhibitor to an activated product that either decays to product or reacts with the enzyme (N5 of the FAD for these compounds) to form a covalent adduct. This section will discuss the molecular interactions of the three classes of compounds rather than the extensive pharmacological data from rat studies or from the clinic.

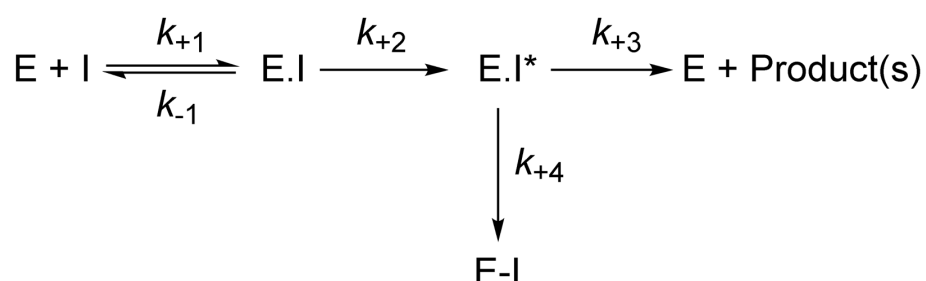


Figure 7 Mechanism-based inhibition of MAO: the reactive product can either dissociate or react to form a covalent adduct.

The original discovery of the antidepressant effect of hydrazines came from the observation of mood elevation in tuberculosis patients treated with isoniazid. Hydrazines were then characterized as effective MAO inhibitors (Zeller *et al.*, 1955). Both phenelzine and isocarboxazid carry the risk of liver toxicity but remain useful for treatment-resistant depression. The reversible inhibition of MAO by phenelzine is poor ( $K_i$  is 47  $\mu\text{M}$  for MAO A, 15  $\mu\text{M}$  for MAO B (Binda *et al.*, 2008)), as it is in rat and pig brain (Tipton and Spires, 1971). Inactivation requires that the hydrazine acts first as a substrate. The product from the oxidation of the hydrazine could be either an imine that is hydrolysed to the aldehyde and released as usual with concomitant  $\text{H}_2\text{O}_2$  production, or the product could be a diazene that reacts with oxygen giving a radical that could alkylate the flavin. Inactivation of MAO A and of MAO B follow the same  $\text{O}_2$  dependent mechanism with some turnover for each inactivation event (the partition ratio). The kinetics of inactivation give  $k_{\text{inact}}/K_{\text{inact}}$  equal to 18  $\text{min}^{-1}\text{M}^{-1}$  for MAO A and 3  $\text{min}^{-1}\text{M}^{-1}$  for MAO, B both with a partition ratio of turnover to inactivation of about 40 (Binda *et al.*, 2008). The crystal structure shows that the adduct formed is at N5 of the FAD (Fig. 4).

Tranylcypromine (TCP) inactivation of MAO has been studied in depth using a variety of cyclopropylamine derivatives. TCP itself modifies the flavin at the C4a position (Fig. 4) but N-cyclo- $\alpha$ -methylbenzylamine modifies a cysteine. Chemical and mechanistic studies of the inactivation

support a radical mechanism in which one electron passes from the substrate amino group to the oxidized flavin to give the amine radical cation and the flavosemiquinone, followed by opening of the cyclopropyl ring and adduct formation (Silverman, 1995). Where adduct formation does not occur, further oxidation gives the iminium ion which can either leave the active site or react with nearby cysteines. Reversible inhibition by TCP is weak at around 100  $\mu\text{M}$  for both MAO A and B (Table 5) (Bonivento *et al.*, 2010, Malcomson *et al.*, 2015). Inactivation with low partition ratios in both forms, is marginally better in MAO B ( $k_{\text{inact}}/K_{\text{inact}}$  is 0.2 compared to 0.1  $\text{min}^{-1} \cdot \mu\text{M}^{-1}$  in MAO A). Interestingly, in MAO B the covalently bound TCP stabilizes the entrance cavity residues to favour binding of 2-BFI, an imidazoline site ligand (Bonivento *et al.*, 2010, McDonald *et al.*, 2010). The clinical pharmacology for tranylcypromine use in depression has recently been reviewed in a meta-analysis which found that, when administered with dietary restriction of tyramine, it is a safe and effective antidepressant (Ricken *et al.*, 2017).

**Table 5** Kinetic parameters for initial binding and for inactivation of MAO by irreversible inhibitors.

Compound	MAO A			MAO B		
	$K_i$ ( $\mu\text{M}$ )	$K_{\text{inact}}$ ( $\mu\text{M}$ )	$k_{\text{inact}}$ ( $\text{min}^{-1}$ )	$K_i$ ( $\mu\text{M}$ )	$K_{\text{inact}}$ ( $\mu\text{M}$ )	$k_{\text{inact}}$ ( $\text{min}^{-1}$ )
Phenelzine	47	3.1	0.12	15	0.9	0.9
Tranylcypromine	91	7.7	0.77	105	0.16	0.16
Pargyline	15	22	0.65	1.8	0.35	0.35
Deprenyl	75	193	0.25	0.97	103	0.53

The propargylamine class of inactivators provides clear examples of the importance of initial ligand binding in selectivity, as seen in the 100-fold better  $K_i$  for deprenyl on MAO B than for MAO A (Table 5). As with both the hydrazines and cyclopropylamines, the first step in inactivation by propargylamines is the mechanism-based oxidation to the propargylimine. With the product retained in the active site by the positive charge, the allenyl resonance form undergoes nucleophilic attack by the  $\text{FADH}^-$  forming a substituted 1,3-diaminoallene which, mediated by a water molecule, rearranges to the final delocalized product. The stable adduct to N5 (Fig. 4) is the same for all propargylamines studied (Binda *et al.*, 2005, Albrecht *et al.*, 2018). The rate constants for inactivation ( $k_{\text{inact}}$ ) are similar in MAO A and MAO B (Table 5) but the  $K_{\text{inact}}$  values reflect the selectivity of pargyline and deprenyl for MAO B inactivation. An even bigger selectivity difference is seen in the partition ratios for

deprenyl: 482 in MAO A but only 1 for MAO B, indicating that every oxidation results in adduct formation in MAO B but that 482 product molecules are released from MAO A for each inactivation event. Thus, design of the optimum propargylamine inactivator must consider initial binding, oxidation rate and product retention and reactivity with the reduced flavin.

In the propargylamine class, pargylamine has been in clinical use longest but deprenyl now leads the market as adjunct therapy for Parkinson's disease. The highly MAO A selective clorgyline and MAO B selective deprenyl are used in PET scans (Fowler *et al.*, 2015a). It must be noted that, under chronic administration of higher doses, each of these selective inactivators will inactivate the other form of the enzyme (Fowler *et al.*, 2015b).

## 6. Computational innovation

The irreversible inhibitors are clinically important and the propargylamine moiety is of particular interest for combination into multi-target drugs (see below). Advance drug design is facilitated by good crystal structures, by mechanistic understanding and by large datasets of tested compounds as well as libraries of fragments to allow discovery of novel compounds to inhibit the enzyme. The rapid expansion of computational power to analyze large data and development of algorithms and programs techniques to explore the information has provided major advances in the last 10 years.

### 6.1 Theoretical elucidation of mechanism

Insight into the mechanism has come from transition state theory using multiscale simulations to calculate the free energy barriers for the catalytic step in the oxidation of amines by MAO (reviewed in (Vianello *et al.*, 2016)). The lower the free energy barriers between substrate, transition state intermediate, and product, the faster the reaction. The highest resolution structure of MAO was optimized, fitted to the electrostatic potential, and the solvent reaction field included, then EVB calculations applied to the oxidation of a substrate such as dopamine by lumiflavin in the gas phase compared to the reaction in the enzyme. The work revealed that dopamine is stripped of its proton (pKa 8.3) for the catalytic reaction that requires the neutral amine before oxidation via a two-step hydride transfer in which H<sup>-</sup> (one proton and two electrons) is transferred to the N5 of the flavin and the other H<sup>+</sup> is removed from the substrate nitrogen and transferred via a water relay to N1 of the flavin to yield the neutral product required for dissociation. The calculated energy for the reaction was 16.1 kcal/mol in good agreement with the experimentally determined 16.5 kcal/mol. The method not only provides insight into the mechanism but also provides information relevant to design of the propargylamine inactivators of MAO. As described above, these mechanism-based inhibitors are first oxidized as substrates generating a positively charged product that could be retained close to the reduced flavin by electrostatic attraction and by favorable cation- $\pi$  interactions in the active site "aromatic cage", where it can react with the reduced flavin to form a covalent adduct (Albrecht *et al.*,

2018).

## 6.2 Data-mining and tools for drug discovery

By far the most important computational advance for drug discovery has been the ability to search databases of millions of compounds for “hits” – compounds with a pharmacophore that will have good affinity for a target binding site. With a clinically and biologically validated target identified, crystallized proteins and proven ligands enable the development of the descriptors for key interactions with the target binding site. The pharmacophore derived from effective, selective molecules allows chemi-informatics to identify similarity-based compounds and, with advanced data-mining, to exclude binding to undesirable off-targets (Nikolic *et al.* , 2015). The dual resource of ligand and target information provides the basis for virtual screening that is now routine in drug discovery. Objective ranking of the hits can then be achieved by docking and model refinement. Molecular dynamics to check the ligand to protein fit is also important, allowing for the target flexibility, and subsequent optimization of the ligand structure. A much shorter list must then be synthesized and experimentally verified. The process has recently been summarized with examples across target fields (Ramsay *et al.* , 2018).

To address the failure rate between ligand and drug, many computation approaches have been developed for the optimization of druggability, blood-brain barrier penetration, lipophilicity, and metabolism. All the computational approaches contribute to more cost-effective discovery and optimization of compounds, accelerating progress toward the clinic. Such high-throughput methods with the power to consider multiple targets at the same time are particularly effective and useful for designing multi-target drugs as will be considered in the next section.

## 7 Conclusion: the future for MAO inhibition in multi-target drugs

The concept of multi-target drugs (MTD) to treat complex, multifactorial diseases such as neurodegeneration and cancer emerging at the beginning of this century. By 2017, 21% of the new compounds approved by the US Food and Drug Administration (FDA) for clinical use were aimed at more than one target, a testament to the rapid progress facilitated by computational approaches and high through-put technology as well as the progress in target identification and assay development at the experimental level, drugs against cancer and neuropathologies were the largest classes of these MTD (Ramsay *et al.*, 2018). MAOI with their proven effects of slowing the breakdown of neurotransmitters are a key part of the anti-neurodegenerative MTD.

Examples of MTD already on the market include inhibitors of neurotransmitter reuptake systems (SNRIs) and antagonists for combinations of receptors such the dopamine D2, serotonin 5-HT2A and  $\alpha$ 1-adrenergic receptors that can treat schizophrenia. For the brain, the main enzyme targets for recent

compound discovery have been the cholinesterases (ChE) that modulate release of other neurotransmitters, the monoamine oxidases (MAO) to elevate levels of monoamines, and beta-secretase 1 (BACE1) to decrease the generation of the toxic amyloid beta (A $\beta$ ) peptide. One compound that has been studied in phase 2 clinical trials for cognitive impairment is ladostigil which combines two pharmacophores taken from rivastigmine (a ChE inhibitor) and rasagiline (a propargylamine inactivator of MAO). Ladostigil inhibits acetylcholinesterase, butyrylcholinesterase, and monoamine oxidases A and B, and has neuroprotective effects (reviewed in (Finberg and Rabey, 2016)). The main dilemma in the design of multi-target drugs is choosing the correct targets, and finding the correct balance of potency for all targets in one compound in order to have the desired effect *in vivo*.

Although inhibition of the enzyme catalyts decreases turnover, inhibition of receptors stops cascading of signals. This led to the design of a tripotent compound to inhibit known enzyme targets (ChE and MAO) that also blocks the histamine receptor H3, inhibition of which is known to elevate acetylcholine, serotonin, dopamine and norepinephrine in the central nervous system. The resulting tripotent compound, contilisant, may be a useful MTD in neurodegenerative diseases (Bautista-Aguilera *et al.* , 2017).

Medicinal chemical approaches, facilitated by computation, will provide many more similar candidates in the future. However, pharmacology to identify and validate the correct targets remains the key step in getting the correct compounds into clinical trials and on towards the market.

## References

- Albrecht A., Vovk I., Mavri J., Marco-Contelles J., Ramsay R. R., *Frontiers in Chemistry*, **6** (2018), 169.
- Anderson M. C., Hasan F., McCrodden J. M., Tipton K. F., *Neurochem. Res.*, **18** (1993), 1145-1149.
- Bailey K. R., Ellis A. J., Reiss R., Snape T. J., Turner N. J., *Chem. Commun.*, (2007), 3640-2.
- Bautista-Aguilera O. M., Hagenow S., Palomino-Antolin A., Farré-Alins V., Ismaili L., Joffrin P.-L., et al., *Ang Chem*, **56** (2017), 12765–12769
- Becchi S., Buson A., Foot J., Jarolimek W., Balleine B. W., *Brit. J. Pharmacol.*, **174** (2017), 2302-2317.
- Benedetti M. S., Tipton K. F., Whomsley R., *Fundam. Clin. Pharmacol.*, **15** (2001), 75-84.
- Binda C., Hubalek F., Li M., Herzig Y., Sterling J., Edmondson D. E., et al., *J Med Chem*, **48** (2005), 8148-8154.
- Binda C., Li M., Hubalek F., Restelli N., Edmondson D. E., Mattevi A., *Proc. Natl. Acad. Sci. U.S.A.*, **100** (2003), 9750-9755.
- Binda C., Newton-Vinson P., Hubalek F., Edmondson D. E., Mattevi A., *Nature Structural Biology*, **9** (2002), 22-26.
- Binda C., Wang J., Li M., Hubalek F., Mattevi A., Edmondson D. E., *Biochemistry*, **47** (2008), 5616-5625.
- Binda C., Wang J., Pisani L., Caccia C., Carotti A., Salvati P., et al., *J Med Chem*, **50** (2007), 5848-5852.
- Bonivento D., Milczek E. M., McDonald G. R., Binda C., Holt A., Edmondson D. E., et al., *J. Biol. Chem.*, **285** (2010), 36849-36856.
- Borstnar R., Repic M., Krzan M., Mavri J., Vianello R., *Eur. J. Org. Chem.*, (2011), 6419-6433.
- Bortolato M., Shih J. C., *Intl. Rev. Neurobiol.*, **100** (2011), 13-42.
- Caccia C., Maj R., Calabresi M., Maestroni S., Faravelli L., Curatolo L., et al., *Neurology*, **67** (2006), S18-S23.
- Carradori S., Secci D., Petzer J. P., *Expert Opin Ther Pat*, **28** (2018), 211-226.
- Checknita D., Maussion G., Labonte B., Comai S., Tremblay R. E., Vitaro F., et al., *Brit. J. Psychiatry*, **206** (2015), 216-222.
- Curet O., Damoiseau G., Aubin N., Sontag N., Rovei V., Jarreau F. X., *Journal of Pharmacology and Experimental Therapeutics*, **277** (1996), 253-264.
- Da Prada M., Kettler R., Keller H. H., Burkard W. P., Muggli-maniglio D., Haefely W. E., *Journal of Pharmacology and Experimental Therapeutics*, **248** (1989), 400-414.
- De Colibus L., Li M., Binda C., Lustig A., Edmondson D. E., Mattevi A., *Proc. Natl. Acad. Sci. U.S.A.*, **102** (2005), 12684-12689.
- Delpont A., Harvey B. H., Petzer A., Petzer J. P., *Toxicol. App. Pharmacol.*, **325** (2017), 1-8.

Edmondson D. E., Binda C., Mattevi A., *Arch Biochem Biophys*, **464** (2007), 269-276.

Erickson J. D., Schafer M. K., Bonner T. I., Eiden L. E., Weihe E., *Proc. Natl. Acad. Sci. U.S.A.*, **93** (1996), 5166-5171.

Finberg J., Rabey J., *Front. Pharmacol.*, **7** (2016), 340.

Finberg J. P. M., Gillman K., *Intl. Rev. Neurobiol.*, **100** (2011), 169-190.

Fowler C. J., Tipton K. F., *J. Pharm. Pharmacol.*, **36** (1984), 111-115.

Fowler J. S., Logan J., Shumay E., Alia-Klein N., Wang G.-J., Volkow N. D., *J Labelled Compounds & Radiopharmaceuticals*, **58** (2015a), 51-64.

Fowler J. S., Logan J., Volkow N. D., Shumay E., McCall-Perez F., Jayne M., et al., *Neuropsychopharmacol.*, **40** (2015b), 650-657.

Fowler J. S., Logan J., Volkow N. D., Wang G. J., *Molecular Imaging and Biology*, **7** (2005), 377-387.

Gillman P. K., *Anaesthesia*, **61** (2006), 1013-1014.

Gillman P. K., *Journal of Psychopharmacology*, **25** (2011), 429-436.

Hubalek F., Binda C., Khalil A., Li M., Mattevi A., Castagnoli N., et al., *J. Biol. Chem.*, **280** (2005), 15761-15766.

Hynson R., Kelly S., Price N., Ramsay R., *Biochim. Biophys. Acta*, **1672** (2004), 60-66.

Jones T. Z. E., Giurato L., Guccione S., Ramsay R. R., *FEBS J*, **274** (2007), 1567-1575.

Kar S., Leszczynski J., *Current Drug Metabolism*, **18** (2017), 1106-1122.

Kay C. W. M., El Mkami H., Molla G., Pollegioni L., Ramsay R. R., *Journal of the American Chemical Society*, **129** (2007), 16091-16097.

Kim H., Sablin S., Ramsay R., *Arch Biochem Biophys*, **337** (1997), 137-142.

Krueger M. J., Mazouz F., Ramsay R. R., Milcent R., Singer T. P., *Biochemical and Biophysical Research Communications*, **206** (1995), 556-562.

Li M., Hubalek F., Newton-Vinson P., Edmondson D. E., *Protein Expression and Purification*, **24** (2002), 152-162.

Lum C. T., Stahl S. M., *CNS Spectrums*, **17** (2012), 107-120.

Ma J. C., Yoshimura M., Yamashita E., Nakagawa A., Ito A., Tsukihara T., *J Mol Biol*, **338** (2004), 103-114.

Malcomson T., Yelekci K., Borrello M. T., Ganesan A., Semina E., De Kimpe N., et al., *FEBS J*, **282** (2015), 3190-3198.

Manca M., Pessoa V., Lopez A. I., Harrison P. T., Miyajima F., Sharp H., et al., *J. Mol. Neurosci.*, **64** (2018), 459-470.

Mattevi A., *TIBS*, **31** (2006), 276-283.

McDonald G. R., Olivieri A., Ramsay R. R., Holt A., *Pharmacological Research*, **62** (2010), 475-488.

Medvedev A. E., Ramsay R. R., Ivanov A. S., Veselovsky A. V., Shvedov V. I., Tikhonova O. V., et al., *Neurobiology*, **7** (1999), 151-158.

Milczek E. M., Binda C., Rovida S., Mattevi A., Edmondson D. E., *FEBS J*, **278** (2011), 4860-4869.

Mosharov E. V., Larsen K. E., Kanter E., Phillips K. A., Wilson K., Schmitz Y., et al., *Neuron*, **62** (2009), 218-29.

Mosharov E. V., Staal R. G., Bove J., Prou D., Hananiya A., Markov D., et al., *J. Neurosci.*, **26** (2006), 9304-11.

Newton-Vinson P., Hubalek F., Edmondson D. E., *Protein Expression and Purification*, **20** (2000), 334-345.

Nikolic K., Mavridis L., Bautista-Aguilera O. M., Marco-Contelles J., Stark H., Carreiras M. D., et al., *J Comput Aid Mol Des*, **29** (2015), 183-198.

Nutt D. J., *J. Clin. Psychiatry*, **67 Suppl 6** (2006), 3-8.

Orru R., Aldeco M., Edmondson D. E., *J. Neural Transm.*, **120** (2013), 847-851.

Pena-Silva R. A., Miller J. D., Chu Y., Heistad D. D., *Am. J. Physiol: Heart & Circ. Pysiol.*, **297** (2009), H1354-H1360.

Pinsonneault J. K., Papp A. C., Sadee W., *Human Mol. Genet.*, **15** (2006), 2636-2649.

Ramadan Z. B., Wrang M. L., Tipton K. F., *Neurochemical research*, **32** (2007), 1783-90.

Ramsay R. R., *J. Neural Transm.*, **52** (1998), 139-147.

Ramsay R. R., Dunford C., Gillman P. K., *Brit. J. Pharmacol.*, **152** (2007), 946-951.

Ramsay R. R., Hunter D. J. B., *Biochimica Et Biophysica Acta-Proteins and Proteomics*, **1601** (2002), 178-184.

Ramsay R. R., Olivieri A., Holt A., *J. Neural Transm.*, **118** (2011), 1003-1019.

Ramsay R. R., Popovic-Nikolic M. R., Nikolic K., Uliassi E., Bolognesi M. L., *Clin. Transl. Med.*, **7** (2018), 3.

Ramsay R. R., Tipton K. F., *Molecules (Basel, Switzerland)*, **22** (2017).

Rendic S., Guengerich F. P., *Chem. Res. Toxicol.*, **28** (2015), 38-42.

Reniers J., Meinguet C., Moineaux L., Masereel B., Vincent S. P., Frederick R., et al., *European journal of medicinal chemistry*, **46** (2011), 6104-6111.

Ricken R., Ulrich S., Schlattmann P., Adli M., *European neuropsychopharmacology : the journal of the European College of Neuropsychopharmacology*, **27** (2017), 714-731.

Sablin S. O., Ramsay R. R., *Antiox. Redox Sign.*, **3** (2001), 723-729.

Sablin S. O., Yankovskaya V., Bernard S., Cronin C. N., Singer T. P., *Eur. J. Biochem.*, **253** (1998), 270-279.

Sabol S. Z., Hu S., Hamer D., *Human Genet.*, **103** (1998), 273-279.

Salach J. I., *Arch Biochem Biophys*, **192** (1979), 128-137.

Shih J. C., Wu J. B., Chen K., *J. Neural Transm.*, **118** (2011), 979-986.

Shumay E., Logan J., Volkow N. D., Fowler J. S., *Epigenetics*, **7** (2012), 1151-1160.

Silverman R. B., *Accounts of Chemical Research*, **28** (1995), 335-342.

Singer T. P., Ramsay R. R., *FEBS Letters*, **274** (1990), 1-8.

Son S. Y., Ma A., Kondou Y., Yoshimura M., Yamashita E., Tsukihara T., *Proc. Natl. Acad. Sci. U.S.A.*, **105** (2008), 5739-5744.

Stefanachi A., Leonetti F., Pisani L., Catto M., Carotti A., *Molecules (Basel, Switzerland)*, **23** (2018).

Stocchi F., Vacca L., Grassini P., De Pandis M. F., Battaglia G., Cattaneo C., et al., *Neurology*, **67** (2006), S24.

Tan A. K., Ramsay R. R., *Biochemistry*, **32** (1993), 2137-2143.

Tipton K. F., *J. Neural Transm.*, (2018).

Tipton K. F., Spires I. P. C., *Biochem. J.*, **125** (1971), 521-524.

Tripathi A. C., Upadhyay S., Paliwal S., Saraf S. K., *Eur. J. Med. Chem.*, **145** (2018), 445-497.

van Amsterdam J., Talhout R., Vleeming W., Opperhuizen A., *Life Sci.*, **79** (2006), 1969-1973.

Vianello R., Domene C., Mavri J., *Front. Neurosci.*, **10** (2016).

Vianello R., Repic M., Mavri J., *Eur. J. Org. Chem.*, (2012), 7057-7065.

Weyler W., Titlow C. C., Salach J. I., *Biochem. Biophys. Res. Commun.*, **173** (1990), 1205-1211.

Wouters J., *Curr. Med. Chem.*, **5** (1998), 137-162.

Youdim M. B. H., Edmondson D., Tipton K. F., *Nat. Rev. Neurosci.*, **7** (2006), 295-309.

Zapata-Torres G., Fierro A., Barriga-Gonzalez G., Cristian Salgado J., Celis-Barros C., *J. Chem. Inf. Model.*, **55** (2015), 1349-1360.

Zeller E. A., Barsky J., Berman E. R., *J. Biol. Chem.*, **214** (1955), 267-74.